A Fully 4D Expectation Maximization Algorithm Using Gaussian Diffusion Based Detector Response for Slow Camera Rotation Dynamic SPECT [1]

T. H. Farncombe[†], M. A. King[†], A. M. Celler[‡], S. Blinder[‡]
[†] Department of Nuclear Medicine, University of Massachusetts Medical School, Worcester, MA, USA
[‡] Division of Nuclear Medicine,Vancouver Hospital and Health Sciences Centre, Vancouver, B.C., Canada

Abstract

The dynamic expectation maximization algorithm (dEM) has been developed to determine the kinetic information of various metabolic processes from SPECT projection data acquired with a single slow camera rotation. Depth-dependent detector response compensation (DRC) has been tested as a means to improve the accuracy of these reconstructions. As well, by limiting the number of temporal frames in a dSPECT reconstruction, it is hoped that improved image quality will result. With this reduction in temporal frames, it becomes possible to use block-iterative type reconstruction methods to decrease reconstruction time.

To test the effect of DRC in the dEM algorithm, a series of computer simulations have been performed using the dMCAT phantom modified to model the kinetic response to Tc-99m Teboroxime. Reconstructions indicate that the inclusion of three dimensional DRC with the dEM algorithm improves image quality compared to no DRC. Furthermore, dynamic reconstructions are able to provide additional information, namely kinetic parameters, not attainable with static reconstruction methods. A reduction in the number of temporal frames reconstructed resulted in slightly increased image quality and time activity curve accuracy, but at the expense of decreased temporal resolution. Such a reduction may be acceptable if the temporal changes present are not great compared to the data acquisition time.

I. Introduction

In a conventional SPECT study, it is possible for the distribution of the radiotracer within the body to change over the acquisition time. If such a temporal change is significant, inconsistent projection measurements will result when acquired with a conventional slow camera rotation [1]. Often such a temporal change may be the result of physiologcal changes in the body related to organ function and as such, may provide information useful for diagnostic purposes. In order to obtain estimates of these dynamic processes, dynamic SPECT using multiple fast rotations of a SPECT camera has often been used in the past [2]. However, such data collection often results in a low signal to noise ratio, thus resulting in poor reconstructed images. Alternative methods of dynamic SPECT have been proposed that produce tomographic kinetic information, while maintaining a conventional slow camera rotation. We will denote such a data acquisition technique as dSPECT (dynamic SPECT) and will present in this paper, improvements to the dynamic expectation maximization algorithm (dEM) for determining the temporal behaviour of activity within an object from data acquired in such a manner.

In our method of dSPECT, temporal changes in the radiotracer distribution within an object are represented in terms of linear inequality constraints over time [3]. Once transformed into this representation, it is possible to use a modified version of the expectation maximization algorithm in order to reconstruct the changes in activity that occur over the data acquisition time.

In conventional SPECT, it has been determined that in most cases, improvements in reconstruction accuracy and lesion detectability result when the 3D depth-dependent nature of SPECT spatial resolution is taken into account in the reconstruction process [4]. This aids the reconstruction by making the projection data more consistent as each object voxel is sampled over a number of detector elements at each projection angle. This is similarly the case in dSPECT and it has been shown that reconstruction accuracy improves when multiple projection angles are acquired simultaneously at the same time point [3]. Thus, the inclusion of 3D detector response compensation (DRC) into the dEM algorithm should result in improved dSPECT reconstruction quality, and hence more accurate kinetic estimates.

Because of the rather large computational demand involved in reconstructing a dynamic SPECT data set, previous implementations of the dEM algorithm have focused on reconstructing transverse slices with depth-dependent detector-response within each slice only. As well, at each projection angle, a separate radiotracer distribution was reconstructed. While such a method results in high temporal resolution, this quickly produces an overabundance of data when reconstructed with fully 4D methods (eg., $64 - 128 \times 128 \times 128$ images $\approx$ 500MB of data). Because of this, when a high degree of temporal resolution is not required, it would be advantageous to reduce the number of temporal frames reconstructed. As well as reducing computer requirements, this should provide improved image quality as the data from each temporal frame is better supported across a subset of projection angles. Computation time can also be reduced in this scenerio as it allows for block-iterative reconstruction methods to be used as we shall see.

II. Dynamic Expectation Maximization

The dEM algorithm [5] reconstructs a series of three dimensional spatial images of the tracer distribution within the object. For example, from dSPECT projection data acquired of

[1]This work was supported in part by grant number HL 50349 from the National Heart, Lung and Blood Institute

a $128 \times 128 \times 128$ object over 64 projections, the current dEM algorithm reconstructs 64 different $128 \times 128 \times 128$ images, where each image corresponds to one of the 64 time frames when a projection was acquired.

A. Linear Inequality Temporal Constraints

For a given object voxel, any change in activity from one time frame to the next can be represented in terms of the activity difference over the time frames. Two possibilities exist for how the activity can vary over two consecutive time frames. These are:

i) Decreasing activity from one frame to the next.

$$x_0 \geq x_1 \geq 0 \quad or \quad x_0 - x_1 \geq 0 \tag{1}$$

ii) Increasing activity from one frame to the next.

$$0 \leq x_0 \leq x_1 \quad or \quad x_1 - x_0 \geq 0 \tag{2}$$

In both cases, the differences have been written so as to provide a positive quantity. As well, when the difference between two consecutive time frames is equal to zero, we have $x_0 = x_1$ (ie., static behaviour). Over all J time frames, we can denote the differences in activity within the kth voxel as the vector $\tilde{\mathbf{x}}_\mathbf{k}$, and relate it to the voxel activity $\mathbf{x_k}$ by the matrix-vector product,

$$\tilde{\mathbf{x}}_\mathbf{k} = A_k \mathbf{x_k} \tag{3}$$

where A_k is a matrix of size $(J \times J)$ and $\mathbf{x_k}$ and $\tilde{\mathbf{x}}_\mathbf{k}$ are vectors of length J, representing the activity and the activity difference respectively, within the kth object voxel over the J time frames. It should be pointed out that each object voxel will have a corresponding difference matrix A_k, which can then be combined together in a large matrix A for the entire object.

The simple temporal constraints of (1) and (2) are sufficient to describe a variety of clinical circumstances (eg., washout from the kidneys, accumulation in the liver or bladder, etc.) [6], but they are not able to describe other cases comprised of a combination of both increasing and decreasing behaviour. For such cases, it is possible to formulate a difference matrix by using a combination of (1) and (2) that, when operating on the activity vector, will produce positive activity differences at each time and with the desired overall temporal behaviour. With a temporal link established through the use of the linear inequality temporal constraints, we can now turn our attention to determining the activity difference vector $\tilde{\mathbf{x}}_\mathbf{k}$. For this, we will make use of iterative reconstruction methods, particularly the expectation maximization algorithm [7], although it will be seen that any non block-iterative reconstruction method (eg., ART, MART, etc) will suffice at this point.

B. Dynamic Projection Operator

In the conventional expectation maximization (EM) algorithm, a forward projection operator is applied to the estimated activity distribution within the object at each projection angle. This estimated projection is then compared to the actual collected data for the same angle and then backprojected into the object space in order to arrive at a scaling factor for each object voxel. Mathematically, the projection and backprojection operations can be written as matrix-vector products so that the EM algorithm for SPECT can be written,

$$x_k^{n+1} = \frac{x_k^n}{\sum_{i,j=1}^{I,J} C_{ijk}} \sum_{i,j=1}^{I,J} \frac{C_{ijk} y_{ij}}{\sum_{k'=1}^{K} C_{ijk'} x_{k'}^n} \tag{4}$$

where x_k represents the estimated activity in the kth object voxel, C_{ijk} is the projection matrix that maps the voxelized three dimensional activity distribution into the two dimensional camera space, and y_{ij} represents the actual measured values in the ith detector element at the jth projection stop. Here the object activity distribution x_k is assumed to remain fixed over all the projection measurements acquired and so the size of the projection operator is $(I * J \times K)$ where I is the number of detector elements, J is the number of projection stops, and K is the number of object voxels in the reconstructed three dimensional object space. The projection operator, C_{ijk} can be written as a matrix comprised of the following:

$$C \quad = \quad \begin{pmatrix} (C_{i1k}) \\ (C_{i2k}) \\ \vdots \\ (C_{iJk}) \end{pmatrix} \tag{5}$$

where the (C_{ijk})'s represent the projection of the kth object voxel into the detector element i at the jth projection angle.

In the dynamic case however, the projection operator is no longer an $(I * J \times K)$ matrix since the object distribution is different at each projection angle, but rather is a $(I * J \times K * J)$ matrix. In the dynamic case, the dynamic projection operator (for a single detector head) can therefore be written as,

$$\tilde{C} \quad = \quad \begin{pmatrix} (C_{i1k}) & 0 & 0 & 0 \\ 0 & (C_{i2k}) & 0 & 0 \\ 0 & 0 & \ddots & 0 \\ 0 & 0 & 0 & (C_{iJk}) \end{pmatrix} \tag{6}$$

The use of a Gaussian diffusion projection matrix for modelling the three dimensional depth dependent camera response has been shown to be both computationally efficient and accurate in static SPECT reconstruction algorithms [4]. For this reason, it was chosen to use this method in order to perform the projection and backprojection steps in the dEM algorithm. Due to space limitations, the reader is directed to [4, 8, 9] for more information on Gaussian diffusion DRC.

C. The Dynamic EM Algorithm

As mentioned previously, for any temporal behaviour, an appropriate linear difference matrix can be obtained so that the difference in activity between any two consecutive time frames will always be a positive quantity. As positivity constraints in the unknown variable are inherent in the expectation

maximization algorithm, it is natural to proceed to use this algorithm in order to solve the dynamic SPECT problem.

Following along the lines of the static EM algorithm (4), a dynamic version can be obtained using the activity differences. Thus, the dEM algorithm can be written as,

$$\tilde{\mathbf{x}}_k^{n+1} = \frac{\tilde{\mathbf{x}}_k^n}{\sum_{i,j=1}^{I,J}(\tilde{C}A^{-1})_{ijk}} \sum_{i,j=1}^{I,J} \frac{(\tilde{C}A^{-1})_{ijk} y_{ij}}{\sum_{k'=1}^{K}(\tilde{C}A^{-1})_{ijk'}\tilde{\mathbf{x}}_{k'}^n} \quad (7)$$

where the vector $\tilde{\mathbf{x}}_k$ is the activity difference vector for the kth voxel and is related to the activity by equation (3). Notice that the projection step is actually a projection of the estimated activity distribution within the object at the appropriate time interval. Following reconstruction, the activity difference vector is converted into the activity vector by $\mathbf{x}_k = A_k^{-1}\tilde{\mathbf{x}}_k$.

Given the amount of data produced in a typical dSPECT scan, it is often desireable to reduce the number of unknown variables in order to reduce computational demands. In order to do this, when a high degree of temporal resolution is not required, the number of frames reconstructed can be reduced by altering the dynamic projection matrix such that the tracer distribution remains constant over a subset of angles. Thus, if the number of projection angles is J, and N is the desired number of temporal frames ($N \leq J$), then over each J/N angles, the object activity vector $\mathbf{x}$ can be held constant. In such a case, the projection matrix can be written,

$$\tilde{C} = \begin{pmatrix} (C_{i1k}) & 0 & 0 & 0 \\ \vdots & 0 & 0 & 0 \\ 0 & \left(C_{i(J/N+1)k}\right) & & \\ 0 & \vdots & 0 & 0 \\ 0 & 0 & \ddots & 0 \\ 0 & 0 & 0 & \vdots \\ 0 & 0 & 0 & (C_{iJk}) \end{pmatrix} \quad (8)$$

Similarly, the sizes of the difference matrix A_k and the activity vector $\mathbf{x_k}$ shrink to $(N \times N)$ and $(N \times 1)$ respectively. As each temporal frame is reconstructed based upon the projection data of a few angles, it is possible to apply block-iterative reconstruction methods at this point in order to decrease reconstruction time, for example, grouping the subsets as $\{(C_{i1k}), (C_{i(J/N+1)k}), ...\}$,$\{(C_{i2k}), (C_{i(J/N+2)k}), ...\}$, etc.

III. Simulations

To test the accuracy of the fully 4D dEM algorithm, simulations were performed using a version of the dMCAT [10] model modified to model the extraction and washout of Tc-99m Teboroxime [11]. Kinetic parameters used in this model were based on those found from compartmental modelling of Teboroxime within canine myocardium [2].

Two scenerios were simulated with the dMCAT consisting of a healthy myocardium and the same myocardium with an anterior wall defect. Projection data starting at 1 min post-injection was created using an analytic projector model of a dual head SPECT camera. Detector heads were placed in the 90° configuration and acquisition proceeded from LAO and RAO to LPO and LAO respectively for each head (ie., 90° rotation per head) in a circular orbit of radius 30 cm. A total of 32 projections per head (20 s per projection) were acquired into 64×64 pixel matrices with a pixel size of 6.25 cm. For both heads, a low energy, high resolution collimator was simulated with a FWHM of 1.59 cm at 30 cm. Noiseless projection data was generated and scaled to 5 million total counts and randomly generated Poisson noise added.

Reconstructions were carried out using the static MLEM and the dEM algorithms both with and without the inclusion of 3D detector response. dEM was used with high temporal resolution using all 32 time frames, as well as with 8 and 16 frames. In all cases, a total of 150 iterations were performed.

IV. Results and Discussion

In Figure 1, the impact of using 3D DRC can be seen on a single short axis slice shown at t = 2 min. Reconstructions were performed both with and without 3D DRC. It is apparent from these reconstructions, that when DRC is applied to a dEM reconstruction, improved images result. In this time frame, it appears that the inferior wall of the myocardium is better distinguished in the DRC reconstruction. Additionally, contamination from the liver into the myocardium also appears to be lessened in the 3D DRC image compared to the no DRC image. In both cases, reconstructed time activity (TA) curves disagree to some extent with true TA behaviours, although the general trend for each organ is obtainable and in fact, the initial fast uptake of tracer into the myocardium is distinguishable in the first two time frames.

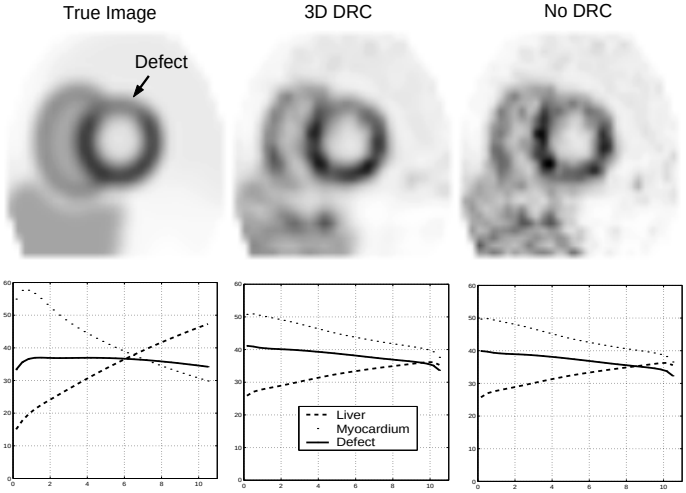

Figure 1: Short axis slice of dMCAT phantom at t = 2 min obtained from dEM reconstruction with and without DRC.

Figure 2 shows sample images of the same short axis slice reconstructed with differing numbers of temporal frames. Images produced from 16 or 8 frames appear very similar, but slight differences can be seen between the dEM and static MLEM reconstructions. At the time frame shown, contrast between the myocardium and the defect appears slightly

greater in the dEM reconstructions compared to the MLEM result. Additionally, the effect of activity uptake into the liver is reduced in dEM vs static reconstructions as the dynamic reconstruction is able to account for the increasing liver activity over time, thus minimizing streak artifacts in the inferior heart wall. Regional TA curves appear very similar in all dEM reconstructions, although the initial fast myocardial uptake is no longer apparent when decreased to 16 temporal frames.

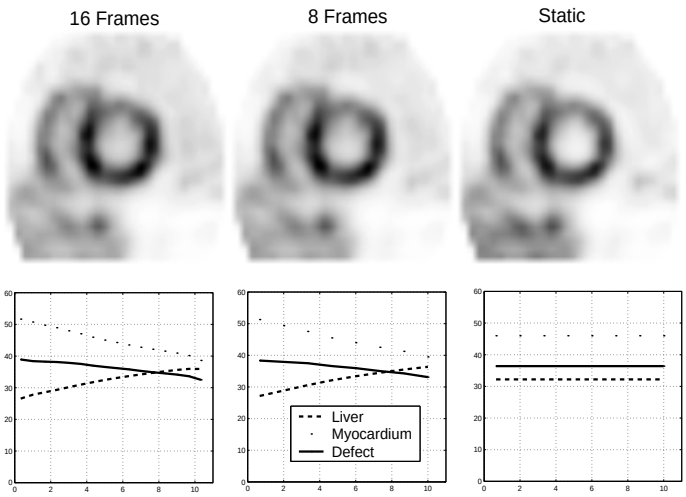

Figure 2: Short axis slice of dMCAT phantom at t = 2 min obtained from dEM reconstruction with fewer temporal frames and with DRC.

It was seen in this simulation that the location of the myocardial defect was able to be determined through both dynamic and static reconstructions. With static methods, images depict an average activity within each object voxel. In this simulation, the data acquisition was started soon enough and was short enough so that the average activity within the myocardium was higher than that in the defect. However, if the acquisition is started later, or if the acquisition time is longer, a static reconstruction may depict the defect with a greater activity, thus giving the appearance of a healthy myocardium. If reconstructed with a dynamic method such a dEM, this effect will not occur as the defect and healthy myocardium can be distinguished based on their dynamic parameters. However, as one decreases the number of temporal frames in a dEM reconstruction, this effect may become more important.

V. Conclusion

A fully 4D dynamic expectation maximization algorithm has been presented for use in dynamic SPECT imaging using slow acquisitions. Depth-dependent spatial resolution is modelled through an incremental Gaussian diffusion, while temporal constraints are enforced in the object at each time frame. These constraints can model a wide range of temporal behaviours, and can be reduced in number in order to decrease reconstruction time and computer requirements. Additionally, reducing temporal frames allows for the possibility of performing an adaptive framing method whereby temporal frames are finely sampled when rapid changes in activity occur and are more coarsely sampled during slow changes.

In computer simulations, the inclusion of DRC in this algorithm has resulted in increased reconstruction accuracy compared with no DRC. As well, by limiting the number of temporal frames in the reconstruction, slightly improved reconstructions result as each reconstructed frame is supported by multiple projection angles. However, one must be cautious of reducing the number of temporal frames too much as a resultant decrease in temporal resolution follows.

VI. References

[1] B. Bok, A. Bice, M. Clausen, D. Wong, and H. Wagner, "Artifacts in camera based single photon emission tomography due to time activity variation," *Eur. J. Nucl. Med.*, vol. 13, pp. 439–442, 1987.

[2] A. Smith, G. Gullberg, P. Christian, and F. Datz, "Kinetic modeling of teboroxime using dynamic SPECT imaging of a canine model," *J. Nuc. Med.*, vol. 35, pp. 484–495, 1994.

[3] T. Farncombe, *Functional Dynamic SPECT Imaging Using a Single Slow Camera Rotation*. PhD thesis, University of British Columbia, 2000.

[4] H. C. Gifford, M. A. King, R. G. Wells, W. G. Hawkins, M. V. Narayanan, and P. H. Pretorius, "LROC analysis of detector-response compensation in SPECT," *IEEE Trans. Med. Imag.*, vol. 19, pp. 463–473, 2000.

[5] T. Farncombe, S. Blinder, A. Celler, D. Noll, J. Maeght, and R. Harrop, "A dynamic expectation maximization algorithm for single camera rotation dynamic SPECT (dSPECT)," *IEEE Nuclear Science Symposium Conference Record*, 2000.

[6] A. Celler, T. Farncombe, C. Bever, D. Noll, J. Maeght, R. Harrop, and D. Lyster, "Performance of the dynamic single photon emission computed tomography (dSPECT) method for decreasing or increasing activity changes," *Phys. Med. Biol.*, vol. 45, pp. 3525–3543, 2000.

[7] L. Shepp and Y. Vardi, "Maximum liklihood reconstruction for emission tomography," *IEEE Trans. Med. Imag.*, vol. MI-1, pp. 113–122, 1982.

[8] A. W. McCarthy and M. I. Miller, "Maximum likelihood SPECT in clinical computation times using mesh-connected parallel computers," *IEEE Trans. Med. Imag.*, vol. 10, pp. 426–436, 1991.

[9] M. A. King, T.-S. Pan, and D.-S. Luo, "An investigation of aliasing with Gaussian-diffusion modelling of SPECT spatial resolution," *Trans. Nucl. Sci.*, vol. 44, pp. 1375–1380, 1997.

[10] P. Pretorius, W. Xia, M. King, B. Tsui, and K. Lacroix, "A mathematical model of motion of the heart for use in generating source and attenuation maps for simulating emission imaging," *Med. Phys.*, vol. 26, pp. 2323–2332, 1999.

[11] A. Celler, S. Blinder, D. Noll, T. Tyler, F. Duclercq, and R. Harrop, "Investigation of the dynamic SPECT (dSPECT) method for teboroxime using a 4-D kinetic thorax model dMCAT," in *Sixth International Meeting on Fully Three-Dimensional Image Reconstruction in Radiology and Nuclear Medicine, submitted*, 2001.